

Pressure dependent excited state dynamics behavior in CzCNDSB

Guang-Jing Hou(侯广静), Ting-Ting Wang(王亭亭), Cun-Fang Feng(冯存方), Hong-Yu Tu(屠宏宇), Yu Zhang(张宇), Fang-Fei Li(李芳菲), Ying-Hui Wang(王英惠), Ping Lu(路萍), Tian Cui(崔田), and Ling-Yun Pan(潘凌云)
Citation: Chin. Phys. B, 2025, 34 (**8**): 087801. DOI: 10.1088/1674-1056/add679
http://cpb.iphy.ac.cn; http://iopscience.iop.org/cpb

What follows is a list of articles you may be interested in

Ultrafast photoemission electron microscopy: A multidimensional probe of nonequilibrium physics

Yanan Dai(戴亚南)
Chin. Phys. B, 2024, 33 (**3**): 038703. DOI: 10.1088/1674-1056/ad174a

Core-level spectroscopy of the photodissociation process of BrCN molecule

Kun Zhou(周坤) and Han Wang(王涵)
Chin. Phys. B, 2024, 33 (**1**): 018702. DOI: 10.1088/1674-1056/ad0cc9

Theoretical investigation on the fluorescent sensing mechanism for recognizing formaldehyde: TDDFT calculation and excited-state nonadiabatic dynamics

Yunfan Yang(杨云帆), Lujia Yang(杨璐佳), Fengcai Ma(马凤才), Yongqing Li(李永庆), and Yue Qiu(邱岳)
Chin. Phys. B, 2023, 32 (**5**): 057801. DOI: 10.1088/1674-1056/ac80af

Ultrafast proton transfer dynamics of 2-(2'-hydroxyphenyl)benzoxazole dye in different solvents

Simei Sun(孙四梅), Song Zhang(张嵩), Jiao Song(宋娇), Xiaoshan Guo(郭小珊), Chao Jiang(江超), Jingyu Sun(孙静俞), and Saiyu Wang(王赛玉)
Chin. Phys. B, 2022, 31 (**2**): 027803. DOI: 10.1088/1674-1056/ac3734

Ultrafast structural dynamics using time-resolved x-ray diffraction driven by relativistic laser pulses

Chang-Qing Zhu(朱常青), Jun-Hao Tan(谭军豪), Yu-Hang He(何雨航), Jin-Guang Wang(王进光), Yi-Fei Li(李毅飞), Xin Lu(鲁欣), Ying-Jun Li(李英骏), Jie Chen(陈洁), Li-Ming Chen(陈黎明), and Jie Zhang(张杰)
Chin. Phys. B, 2021, 30 (**9**): 098701. DOI: 10.1088/1674-1056/ac0baf

---

SPECIAL TOPIC — Structures and properties of materials under high pressure

Pressure dependent excited state dynamics behavior in CzCNDSB

Guang-Jing Hou(侯广静)[1], Ting-Ting Wang(王亭亭)[1], Cun-Fang Feng(冯存方)[2], Hong-Yu Tu(屠宏宇)[1], Yu Zhang(张宇)[1], Fang-Fei Li(李芳菲)[1], Ying-Hui Wang(王英惠)[1], Ping Lu(路萍)[3,†], Tian Cui(崔田)[4,‡], and Ling-Yun Pan(潘凌云)[1,§]

[1] *State Key Laboratory of Superhard Materials, College of Physics, Jilin University, Changchun* 130012, *China*
[2] *College of Chemistry, Jilin University, Changchun* 130012, *China*
[3] *State Key Laboratory of Supramolecular Structure and Materials, Department of Chemistry, Jilin University, Changchun* 130012, *China*
[4] *School of Physical Science and Technology, Ningbo University, Ningbo* 315211, *China*

(Received 13 March 2025; revised manuscript received 7 May 2025; accepted manuscript online 9 May 2025)

High pressure can alter the properties of matter and modulate the excited-state relaxation behavior of materials without chemical intervention. In this study, high pressure was combined with steady-state absorption and fluorescence spectroscopy, as well as transient spectroscopy techniques, to investigate its effect on the optical properties of the stimuli-responsive material (2Z,2′Z)-2,2′-(1,4-phenylene)bis(3-(4-(9H-carbazol-9-yl)phenyl)acrylonitrile) (CzCNDSB). With increasing pressure, the steady-state absorption and fluorescence peaks of CzCNDSB crystals exhibit red shifts, which are fully reversible. At the same time, pressure causes the molecules to pack more closely, leading to an increase in both the number and energy of multiplet self-trapped state, while the energy of local excited state decreases. The steady-state and transient results provide information on electronic energy levels, excited-state dynamics, and other properties of CzCNDSB, which show strong pressure dependence. These findings highlight the potential of CzCNDSB for practical applications such as photodetectors and solar energy conversion.

Keywords: high pressure, CzCNDSB, transient absorption, stimuli-response

PACS: 78.47.jb, 87.15.ht, 62.50.–p, 82.53.–k

DOI: 10.1088/1674-1056/add679 **CSTR:** 32038.14.CPB.add679

1. Introduction

Organic photoelectronic materials have continued to attract widespread attention due to their excellent optoelectronic properties, ease of chemical modification, and diverse material systems. Among them, cyano-substituted p-phenylene propylene and its derivatives represent an important class,[1] which have been widely used in solar cells,[2–4] organic electroluminescent devices,[5,6] field-effect transistors,[7,8] and other applications. Their popularity stems from high luminescence efficiency, excellent thermal stability, and ease of device integration. These molecules have also been found to respond sensitively to external stimuli such as light, electricity, mechanical force, and pH changes,[9–13] making them a class of stimulus-responsive, color-changing materials. The introduction of cyano groups induces a distorted molecular configuration and facilitates the formation of multiple metastable states, often leading to the coexistence of polymorphs.[14–17] The molecular stacking behavior can be determined by crystal structure analysis, and these stimuli-responsive materials provide a valuable platform for exploring the relationship between optoelectronic properties, molecular conformation, and intermolecular stacking. Therefore, it is of great significance to study the stimulus-responsive behavior of cyano-substituted p-phenylene propylene derivatives.

High pressure, as an external stimulus, can alter the structure of matter, induce phase transitions, and generate new materials with unique properties.[18–23] For piezofluorochromic materials (PMs), the high-pressure approach is more efficient than chemical methods due to its simplicity, reversibility, and controllability.

In 2002, Löwe and Weder[24] prepared polymer blends exhibiting stress-responsive color changes from orange-red to blue-green by doping low-density polyethylene with cyano-substituted diphenylvinyl small molecules. In 2012, Dong *et al.*[25] synthesized 9,10-bis((E)-2-(pyrid-2-yl)vinyl)anthracene, which exhibited a fluorescence color change from green to yellow and finally to red under pressure. In 2017, Gautam *et al.*[26] reported another piezoresponsive fluorescent material whose fluorescence peak blueshifted with increasing pressure, resulting in a color change from orange to yellow. Feng *et al.*[27] synthesized a linear molecule, (2Z,2′Z)-2,2′-(1,4-phenylene)bis(3-(4-(9H-carbazol-9-yl)phenyl)acrylonitrile) (CzCNDSB), featuring a highly distorted solid-state confor-

†Corresponding author. E-mail: ply@jlu.edu.cn
‡Corresponding author. E-mail: cuitian@nbu.edu.cn
§Corresponding author. E-mail: lup@jlu.edu.cn

© 2025 Chinese Physical Society and IOP Publishing Ltd. All rights, including for text and data mining, AI training, and similar technologies, are reserved.

mation.It showed excellent reversibility and reproducibility in piezochromic behavior. Shi *et al.*[28] discovered pressure-induced luminescence in the zero-dimensional halogenated chalcogenide material Cs_4PbBr_6. Similar luminescence was observed in the one-dimensional hybrid halogenated chalcogenide $C_4N_2H_{14}SnBr_4$[29] and the two-dimensional halogenated bis-chalcogenide $(CH_3(CH_2)_3NH^{3+})_4AgBiBr_8$ systems.[30] In 2021, the molecular structures dipropoxy-1,4-phenylene)bis(2-(4-(diphenylamino)phenyl)acrylonitrile (TPPA) and dipropoxy-1,4-phenylene)bis(2-(4-(bis(4-methoxyphenyl)amino)phenyl)acrylonitrile (DPMO) were reported.[31] DPMO crystals demonstrated higher pressure sensitivity than TPPA, withstanding up to 10 GPa and exhibiting a fluorescence burst just above 1.6 GPa. DPMO showed a significantly greater sensitivity of 37.5 nm·GPa^{-1}, attributed to its stronger intramolecular charge transfer capability, contributing to its piezochromic response. These studies illustrate that pressure has a profound modulating effect on the excited-state behavior of materials. Investigating the underlying mechanisms can facilitate the development of pressure-responsive materials and broaden the application of pressure as a functional parameter. So far, pressure-dependent photophysical properties of PMs have attracted interest in both steady-state and transient-state studies.

In this paper, we present a systematic study of the pressure-dependent steady-state and transient-state behaviors of the stimuli-responsive material CzCNDSB, using *in situ* high-pressure steady-state absorption and fluorescence spectroscopy, as well as *in situ* high-pressure femtosecond transient absorption spectroscopy. Based on the experimental results, the alternating shifts between multiplet self-trapped state (STS) and local excited (LE) states with changing pressure are proposed as the underlying mechanism for the observed pressure-dependent optical behavior.

2. Experimental methods

2.1. Preparation of materials

CzCNDSB was synthesized according to Ref. [26]. The high-pressure condition was applied using a diamond anvil cell (DAC) device. Silicone oil was used as the pressure-transmitting medium. The chamber had a diameter of 170 μm and a thickness of 62–70 μm.

2.2. Materials analysis

The *in situ* high-pressure ultraviolet-visible (UV-vis) absorption spectroscopy was performed using a light source (Ocean Optics, HL-2000, 360–2400 nm) and a spectrometer (AvaSpec-2048×16, 300–1100 nm) as the detector. *In situ* high-pressure fluorescence spectroscopy measurements were carried out with a Horiba Jobin Yvon LabRAM-HR spectrometer using 325 nm excitation. High-pressure ultrafast kinetic measurements were performed using a home-built transient absorption system. The incident laser beam (800 nm, 30 fs, 1 kHz, Spitfire, Spectra-Physics) was split into pump and probe beams by a beam splitter. The two beams were then coaxially focused into the DAC chamber, and the transmitted probe beam was collected by a monochromator (Omni-λ 2003i) equipped with a PMT (Hamamatsu). Finally, the signal was processed by a lock-in amplifier (SR830, Stanford Co.) and input to a computer.

3. Results and discussion

3.1. Steady state spectrum

CzCNDSB is a compound formed by introducing two functional substituents, carbazole groups, at the terminal phenyl rings of the molecule 1,4-bis(1-cyano-2-phenylethenyl)benzene (CNDSB) (Fig. 1). CzCNDSB crystals exhibit a porous, twisted conformation with cavernous channels, providing internal space that allows them to withstand higher external pressures without damage during compression–decompression cycles. The optical properties of CzCNDSB were characterized by pressure-dependent UV-vis absorption and fluorescence spectroscopy. At ambient conditions, the absorption peak of CzCNDSB crystals appears at 465 nm (Fig. 2(a)). With increasing pressure, the absorption peak red-shifts and broadens. When the pressure reaches 10.4 GPa, the absorption peak shifts to 553 nm. Figure 2(c) shows the trend of the absorption peak position of CzCNDSB crystals with increasing pressure, which is consistent with previous reports.[27] The Raman peaks in the 1100–1700 cm^{-1} region, corresponding to molecular structure vibrations, shift to higher frequencies as pressure increases. This indicates a decrease in the energy of the lowest excited state, leading to a red-shift in the optical spectra due to enhanced polarization effects among molecules.[27] As a result, both intermolecular and intramolecular interactions are strengthened, and the overlap of neighboring atomic orbitals increases. This increase in

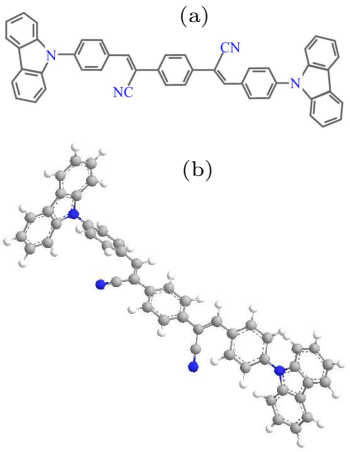


Fig. 1. (a) Two-dimensional and (b) three-dimensional representations of the CzCNDSB molecular structure.

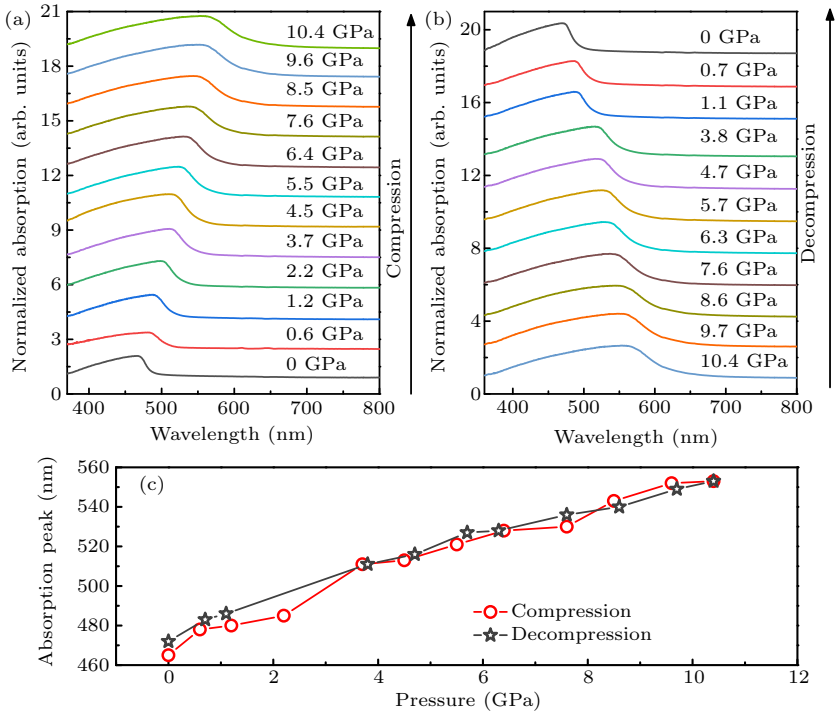


Fig. 2. *In situ* high-pressure steady state absorption spectra of CzCNDSB crystals. (a) Compression process. (b) Decompression process. (c) Trend plot of the absorption peak position with pressure change.

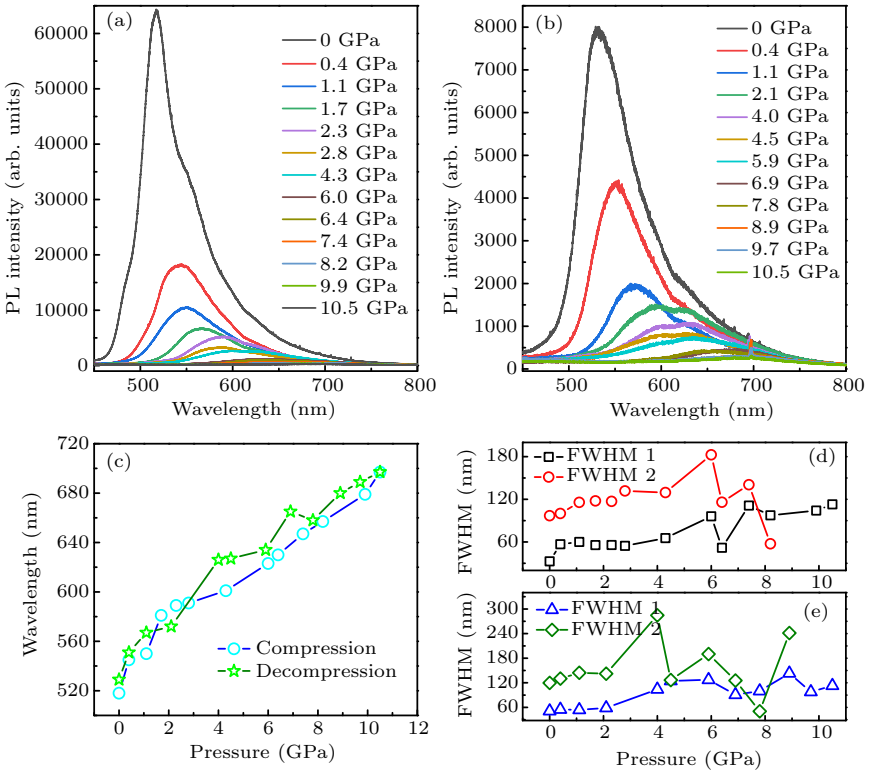


Fig. 3. *In situ* high-pressure fluorescence spectra of CzCNDSB crystals. (a) Compression process. (b) Decompression process. (c) Pressure-dependent trend plot of fluorescence peak position. Trend plots of half-peak width as a function of pressure during (d) compression and (e) decompression.

orbital overlap leads to the dispersion of the conduction and valence band regions, resulting in broader bandwidths and a reduced energy gap. Additionally, Figs. 2(b) and 2(c) show that the variation of the absorption peaks during decompression is nearly identical to that observed during compression, demonstrating the excellent resilience of CzCNDSB crystals.

Figure 3 shows the *in situ* high-pressure fluorescence spectra of CzCNDSB crystals. As the pressure increases, the fluorescence spectra gradually red-shift and the luminescence intensity continuously decreases (Fig. 3(a)). The fluorescence peak is located at 518 nm under ambient conditions. When the pressure reaches 10.5 GPa, the fluorescence peak red-shifts

to 697 nm. Meanwhile, the fluorescence intensity is significantly reduced compared to ambient conditions, and spectra at higher pressures are difficult to observe due to limitations in experimental sensitivity. Therefore, the maximum applied pressure in this study is 10.5 GPa. The decrease in fluorescence intensity is attributed to the enhanced polarization effect among molecules, as previously confirmed by Raman spectroscopy.[27] Subsequently, a slow decompression process was performed to investigate the reversibility of the material (Fig. 3(b)). It was found that the fluorescence spectral shape gradually recovered as the pressure decreased, eventually returning to nearly the same state as before compression, with the fluorescence peak almost returning to its original position. This result indicates good reversibility of the CzCNDSB crystal. Moreover, the fluorescence peak shifts linearly during both compression and decompression processes, suggesting potential applications of the CzCNDSB crystal in pressure sensors and related devices (Fig. 3(c)). Gaussian fitting was performed to further analyze the evolution of molecular energy states. The fluorescence spectra exhibited both long- and short-wavelength components. During the shift of fluorescence peaks, the full width at half maximum (FWHM) of both components nearly doubled under increasing pressure (Figs. 3(d) and 3(e)), suggesting the emergence of a new state. This phenomenon arises from the multiplet STS, which results from decreased molecular spacing.[32,33] The STS is generated by the reduced intermolecular distances in the condensed state and is formed through interactions between the excited state and the adjacent lattice.

3.2. Transient state spectrum

In order to further understand the excited state relaxation dynamics of the CzCNDSB material in response to pressure, time-resolved measurements were performed. A multi-exponential function, $\sum_{i=1}^{n} a_i e^{-t/\tau_i}$, was used to fit the dynamics curves, and the results are shown in Fig. 4(a), where τ_i is the lifetime constant and a_i is the lifetime percentage. The dynamics process can be divided into three components: the <5 ps component corresponding to relaxation from the LE state to the intramolecular charge transfer (ICT) state, the 20–100 ps intraband relaxation component, and the >1 ns relaxation component of the LE state (Figs. 4(b), 4(c), and Table 1). Since the nanosecond time scale obtained from the fitting is close to the delay time limit of the experimental system, only the components with lifetimes <1 ns are discussed here. Under high pressure, the molecular spacing decreases, and the STS, which are the final states of ICT transitions, increase in both number and energy with increasing pressure and become closer to higher excited states. Under these conditions, the molecules move closer to each other, driving the STS to higher energies (Fig. 5).[33,34] The energy of the LE state decreases due to enhanced electronic delocalization. Consequently, the relaxation process from the LE state to the ICT state exhibits an accelerating trend with increasing pressure. These results agree well with previously reported kinetic data.[32–34] The transition observed at 11.5 GPa may be attributed to the interleaving of the STS with the low excited state.

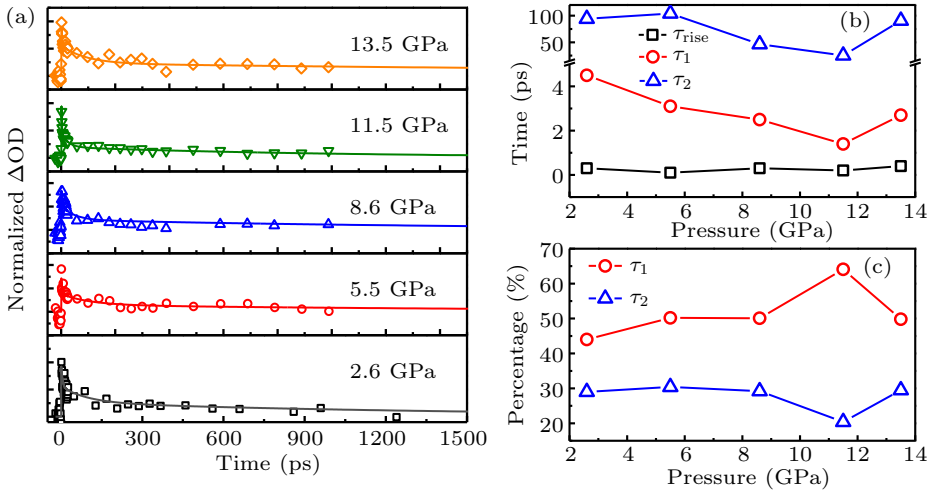


Fig. 4. (a) Normalized dynamic curve of the absorption peak position of CzCNDSB film at different pressures. Plot of (b) decay lifetime and (c) lifetime percentage versus pressure corresponding to the absorption peak position of the CzCNDSB film.

Table 1. Dynamics lifetimes at the absorption peak and lifetime percentage of CzCNDSB films under different pressures.

Pressure (GPa)	τ_1 (ps) (a_1)	τ_2 (ps) (a_2)	τ_3 (ns) (a_3)	τ_{rise} (fs)
2.6	4.5 ± 0.4 (44%)	94.1 ± 2.9 (29%)	1.5 ± 0.2 (27%)	340.0 ± 9.2
5.5	3.1 ± 0.3 (50%)	104.0 ± 4.2 (30%)	1.8 ± 0.5 (20%)	71.9 ± 2.4
8.6	2.5 ± 0.2 (50%)	46.5 ± 5.9 (29%)	1.5 ± 0.2 (21%)	312.0 ± 10.0
11.5	1.4 ± 0.1 (64%)	25.3 ± 0.9 (20%)	1.0 ± 0.1 (16%)	175.7 ± 8.0
13.5	2.7 ± 0.1 (50%)	90.7 ± 5.7 (29%)	3.5 ± 0.6 (21%)	365.2 ± 14.0

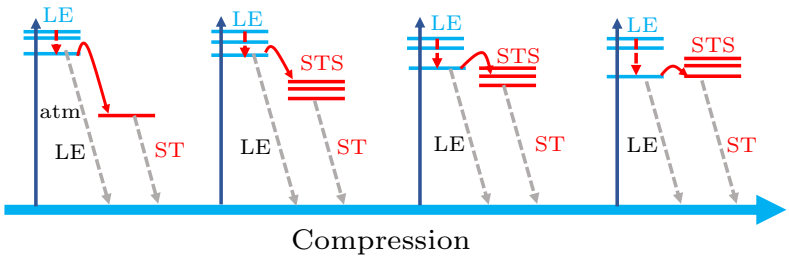


Fig. 5. Schematic representation of the variation of excited state energy levels with pressure in the CzCNDSB molecule. STS: self-trapped state, ST: self-trapped state relaxation, LE (blue): local excited state, and LE (black): local excited state relaxation.

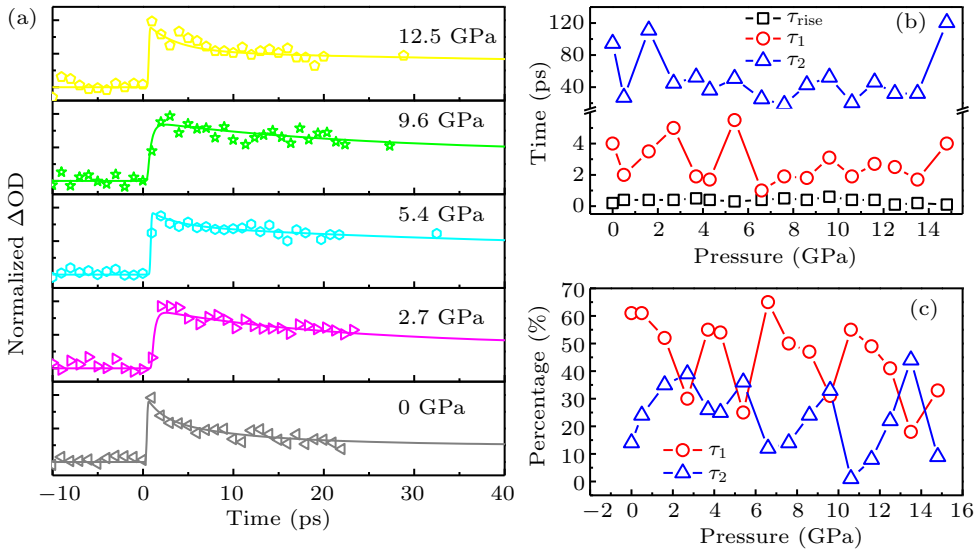


Fig. 6. (a) Normalised dynamic curves of CzCNDSB film at 720 nm for different pressures. Plot of (b) decay lifetime and (c) lifetime percentage versus pressure for CzCNDSB film at 720 nm.

Table 2. Dynamics lifetime and lifetime percentage of CzCNDSB at 720 nm for different pressures.

Pressure (GPa)	τ_1 (ps)	a_1	τ_2 (ps)	a_2	τ_3 (ps)	a_3	τ_4 (ns)	a_4	τ_{rise} (fs)
0	4.0 ± 0.2	61%	94.5 ± 2.9	14%	299.0 ± 4.6	25%			201.9 ± 4.0
0.5	2.0 ± 0.1	61%	27.2 ± 1.1	24%	916.0 ± 4.5	15%			434.8 ± 5.5
1.6	3.5 ± 0.2	52%	111.0 ± 5.4	35%	2868.4 ± 76.2	13%			435.8 ± 3.3
2.7	5.0 ± 0.7	30%	44.7 ± 2.0	39%	1803.2 ± 53.9	31%			422.5 ± 6.3
3.7	1.9 ± 0.1	55%	52.4 ± 2.7	26%	1773.3 ± 46.4	19%			499.4 ± 6.0
4.3	1.7 ± 0.4	54%	36.2 ± 0.2	25%	1058.5 ± 35.3	21%			429.3 ± 4.8
5.4	5.5 ± 0.6	25%	50.8 ± 4.7	36%	401.7 ± 4.4	5%	2.0 ± 0.4	34%	318.5 ± 7.8
6.6	1.0 ± 0.1	65%	25.3 ± 0.6	12%	71.5 ± 2.2	6%	2.0 ± 0.3	17%	448.1 ± 9.3
7.6	1.9 ± 0.2	50%	18.2 ± 3.6	14%	172.8 ± 1.3	22%	19.1 ± 3.5	14%	536.7 ± 4.7
8.6	1.8 ± 0.1	47%	42.8 ± 2.2	24%	656.8 ± 3.4	11%	2.1 ± 0.8	18%	418.3 ± 6.1
9.6	3.1 ± 0.4	31%	52.3 ± 7.2	33%	288.0 ± 6.1	1%	1.7 ± 0.3	35%	591.7 ± 4.4
10.6	1.9 ± 0.2	55%	20.4 ± 1.0	1%	45.5 ± 3.4	22%	1.6 ± 0.2	22%	392.7 ± 3.4
11.6	2.7 ± 0.2	49%	46.2 ± 2.5	8%	113.0 ± 2.0	8%	1.0 ± 0.1	35%	445.0 ± 2.0
12.5	2.5 ± 0.2	41%	31.9 ± 5.5	22%	264.7 ± 4.7	21%	226.4 ± 4.8	16%	132.1 ± 1.5
13.5	1.7 ± 0.6	18%	32.1 ± 3.7	44%	612.3 ± 5.6	23%	6.3 ± 1.5	15%	196.6 ± 3.5
14.8	4.0 ± 1.1	33%	120.5 ± 4.3	9%	182.5 ± 3.0	18%	164.8 ± 5.8	40%	74.8 ± 1.7

Considering the steady-state absorption and fluorescence spectra, 720 nm was chosen to probe the kinetics of the low excited state. As shown in Fig. 6 and Table 2, the population accumulation process is significantly longer in the LE state compared to the higher excited state (at the absorption peak position). Between 0.5 GPa and 11.6 GPa, the τ_{rise} fluctuates between 300 fs and 600 fs, showing no significant change with pressure when considering systematic dispersion. The < 5 ps component of the LE to ICT state relaxation exhibits a wave-like pattern with pressure, alternating between fast (< 2 ps) and slow (> 3 ps) phases. This corresponds to the rise of the STS and the decline of the LE state with increasing pressure, which are interspersed. Since 720 nm is located at the band edge, the LE state redshifts more than the absorption peak with increasing pressure. Considering the observed wave-like pattern and the kinetic changes at the absorption peak, the STS is a multiplet state, where the anisotropic response of the lattice to pressure is more pronounced in this region than

in others. As a result, the electronic energy bands shift staggeredly relative to individual LE states,[32–35] as illustrated in Fig. 5. By comparing the 20–100 ps component of intraband relaxation across pressures, the results show that except for the pressure interval of 1.6–3.7 GPa, the first two decay time components follow the same trend. The intraband relaxation process is faster when the intersystem crossing rate is higher, which is related to pressure-enhanced electron-phonon coupling strength. When the LE state is close to the STS, the STS can relax quickly via electron-phonon coupling. The opposite trend between the two decay components in the 1.6–3.7 GPa range can be explained by the increased distance between the LE and STS at these pressures, resulting in a lower intersystem crossing rate. However, once the STS states are reached, rapid relaxation remains possible.

4. Conclusion

In summary, we investigated the optical properties of CzCNDSB materials under high pressure. The *in situ* high-pressure steady-state absorption spectra show that with increasing pressure, the absorption peaks of CzCNDSB crystals redshift and broaden, resulting in an increased bandwidth and a decreased energy gap. The fluorescence spectra exhibit a good linear correlation with pressure, and the CzCNDSB crystals demonstrate excellent reversibility. Transient absorption kinetics results reveal that both the number and energy of the multiplet STS increase, while the energy of the LE states decreases with increasing pressure. Combining high-pressure techniques with traditional detection methods provides an effective approach to explore the physical properties of matter under pressure, and these findings have important implications for optoelectronic device applications.

Acknowledgements

This project was supported by the National Key Research and Development Program of China (Grant Nos. 2018YFA0305900 and 2017YFA0403704), the National Natural Science Foundation of China (Grant Nos. 61575079, 51632002, 11804113, and 51720105007), and the Natural Science Foundation of Jilin Province, China (Grant No. 20180101230JC).

References

[1] Zhu L and Zhao Y 2013 *J. Mater. Chem. C* **1** 1059
[2] Yella A, Lee H W, Tsao H N, Yi C, Chandiran A K, Nazeeruddin M K, Diau E W G, Yeh C Y, Zakeeruddin S M and Grätzel M 2011 *Science* **334** 629
[3] Kim J Y, Lee K, Coates N E, Moses D, Nguyen T Q, Dante M and Heeger A J 2007 *Science* **317** 222
[4] Mikroyannidis J A, Kabanakis A N, Sharma S S and Sharma G D 2011 *Adv. Funct. Mater.* **21** 746
[5] Hsu C W, Lin C C, Chung M W, Chi Y, Lee G H, Chou P T, Chang C H and Chen P Y 2011 *J. Am. Chem. Soc.* **133** 12085
[6] Zuniga C A, Barlow S and Marder S R 2011 *Chem. Mater.* **23** 658
[7] Komori T, Nakanotani H, Yasuda T and Adachi C 2014 *J. Mater. Chem. C* **2** 4918
[8] Pauchard M, Swensen J, Moses D, Heeger A J, Perzon E and Andersson M R 2003 *J. Appl. Phys.* **94** 3543
[9] Delaire J A and Nakatani K 2000 *Chem. Rev.* **100** 1817
[10] Lv J, Yin X, Zheng H, Li Y, Li Y and Zhu D 2011 *Luminescence* **26** 185
[11] Yen H J, Lin H Y and Liou G S 2011 *Chem. Mater.* **23** 1874
[12] Gentili P L, Nocchetti M, Miliani C and Favaro G 2004 *New J. Chem.* **28** 379
[13] Zheng C, Pu S, Liu G and Chen B 2013 *Tetrahedron Lett.* **54** 7024
[14] Yoon S J and Park S 2011 *J. Mater. Chem.* **21** 8338
[15] Bock H, Göbel I, Näther C, Havlas Z, Gavezzotti A and Filippini G 1993 *Angew. Chem.* **105** 1823
[16] Domenicano A and Vaciago A 1979 *Acta Crystallogr., Sect. B: Struct. Crystallogr. Cryst. Chem.* **35** 1382
[17] Grabowski Z R, Rotkiewicz K and Rettig W 2003 *Chem. Rev.* **103** 3899
[18] Li T, Wang S, Chen X, Chen C, Fang Y and Yang Z 2024 *Chin. Phys. B* **33** 066401
[19] Jiang S, Zhang J, Wang L, Lin C, Yan S, Liu J, Li A and Tai R 2023 *AIP Adv.* **13** 095018
[20] Karaca E and Errandonea D 2023 *Results Phys.* **50** 106581
[21] Liu P, Xu M, Lv J, Gao P, Huang C, Li Y, Wang J, Wang Y and Zhou M 2022 *Chin. Phys. B* **31** 106104
[22] Wang Y, Wang K, Ma Y, Zhou M, Wang H and Liu G 2021 *J. Phys.-Condes. Matter* **33** 355403
[23] Yin X, Zhang J, Dong W, Nakagawa T, Xia C, Zhang C, Guo W, Chang J and Ding Y 2023 *Chin. Phys. B* **33** 016103
[24] Löwe C and Weder C 2002 *Adv. Mater.* **14** 1625
[25] Dong Y, Xu B, Zhang J, Tan X, Wang L, Chen J, Lv H, Wen S, Li B, Ye L, Zou B and Tian W 2012 *Angew. Chem.* **124** 10940
[26] Gautam P, Yu C P, Zhang G, Hillier V E and Chan J M W 2017 *J. Org. Chem.* **82** 11008
[27] Feng C, Wang K, Xu Y, Liu L, Zou B and Lu P 2016 *Chem. Commun.* **52** 3836
[28] Ma Z, Liu Z, Lu S, Wang L, Feng X, Yang D, Wang K, Xiao G, Zhang L, Redfern S A T and Zou B 2018 *Nat. Commun.* **9** 4506
[29] Shi Y, Ma Z, Zhao D, Chen Y, Cao Y, Wang K, Xiao G and Zou B 2019 *J. Am. Chem. Soc.* **141** 6504
[30] Fang Y, Zhang L, Wu L, Yan J, Lin Y, Wang K, Mao W L and Zou B 2019 *Angew. Chem.-Int. Edit.* **58** 15249
[31] Zhu C, Li C, Wen L, Song Q, Wang K, Lv C and Zhang Y 2021 *New J. Chem.* **45** 12895
[32] Furube A, Murai M, Tamaki Y, Watanabe S and Katoh R 2006 *J. Phys. Chem. A* **110** 6465
[33] Wang T T, Zhang Y, Tu H Y, Han L, Cheng J C, Wang X, Li F F, Pan L Y and Cui T 2021 *Chin. Phys. B* **30** 118201
[34] Matsui A, Ohno T, Mizuno K I, Yokoyama T and Kobayashi M 1987 *Chem. Phys.* **111** 121
[35] Xiao L P, Yang X and Zeng L 2018 *Mol. Simul.* **44** 330